DARU Journal of Pharmaceutical Sciences (2018) 26:57–64
https://doi.org/10.1007/s40199-018-0215-3

RESEARCH ARTICLE

Magnetic delivery of antitumor carboplatin by using PEGylated-Niosomes

Fereshteh Davarpanah[1] · Aliakbar Khalili Yazdi[2] · Mahmood Barani[1] · Mohammad Mirzaei[3] · Masoud Torkzadeh-Mahani[2]

Received: 2 August 2018 / Accepted: 4 September 2018 / Published online: 12 September 2018

Abstract

To improve the efficiency of niosomal drug delivery, here we employed two tactics. First, niosomes were magnetized using Fe_3O_4@SiO_2 mangnetic nanoparticles, and second, their surface was modified by PEGylation. PEGylation was intended for increasing the bioavailability of niosomes, and magnetization was used for rendering them capable of targeting specific tissues. These PEGylated magnetic niosomes were also loaded with Carboplatin, an antitumor drug. Next, these niosomes were studied in terms of size, morphology, zeta potential, and drug entrapment efficiency. Then, the in vitro drug release from these modified niosomes was compared to that of both naked and nonmagnetized niosomes. Interestingly, although loading of naked-niosomes with magnetic particles lead to an increase in the rate of drug release, PEGylation of these magnetized niosomes caused a more sustained drug release. Thus, PEGylation of magnetic niosomes, besides improving their bioavailability, caused a slower and sustained release of the drug over time. Finally, studying the in vitro effectives of niosomal formulations towards MCF-7, a breast cancer cell line, showed that PEGylated magnetic niosomes had a satisfactory toxicity towards these cells in the presence of an external magnetic field. In conclusion, PEGylated magnetic niosomes showed enhanced qualities regarding the controlled release and delivery of drug.

Keywords Niosomes · Magnetic particles · PEGylation · Targeted drug delivery · Carboplatin

Introduction

Niosomes are bilayered vesicles composed of non-ionic surfactants. They have been a desireable drug delivery vehicle due to their simple and uniform preparation, low preparation costs, and relatively high shelf-life [1–3]. Because of these promising properties, niosomes have been used in a broad spectrum of applications ranging from topical and skincare treatments [4, 5], over oral and cancer therapies [6, 7], to gene deliveries [8, 9]. However, to further improve the functionality of niosomes, attentions have been drawn to their relatively lower bioavalibility and fast removal from the bloodstream [10, 11]. Amongst approaches that could be taken to address these issues, targeted delivery of the niosomal formulations as well as their surface modifications could be mentioned [12–15].

Targeted delivery of drugs to the tumor sites is one of the applications of drug delivery systems, including niosomes [10, 16]. So far, multiple tactics for targeting tumor tissues are devised, one of which is the recruitment of the magnetic delivery approaches [15, 17]. However, although the use of magnetic delivery approach for the other vesicular drug delivery systems is well stablished [18–20], magnetization of niosomes is relatively unexplored [14]. In magnetic delivery methods, usually nanoparticles (NPs) with strong magnetic properties are used as the targeting agent [21, 22]. A localised magnetic field is then used to direct the accumulation of magnetized carriers in the target tissues, which in turn in expected to increase the local drug concentration and the overall efficiency of the drug delivery.

Another method for improving the functionality of niosomal drug delivery is to increase their bioavailability through surface

✉ Masoud Torkzadeh-Mahani
mtmahani@gmail.com

[1] Department of Nanochemistry, Faculty of Chemistry, Shahid Bahonar University of Kerman, Kerman, Iran

[2] Department of Biotechnology, Institute of Science, High Technology & Environmental Sciences, Graduate University of Advanced Technology, Haft-Bagh Highway, Kerman 7631133131, Iran

[3] Department of Analytical Chemistry, Faculty of Chemistry, Shahid Bahonar University of Kerman, Kerman, Iran

PEGylation, which is defined as the coating of the exterior of niosomes with long chains of polyethylene glycol (PEG). This process hides niosomes from the immune system, and thus, enables the niosomal vesicles to circulate longer in the bloodstream [3, 13, 23]. Moreover, it has been suggested that the high hydrophilicity of PEG is responsible for attracting a layer of water to the surface of niosomes, which in turn prevents the recognition and removal of niosomes by macrophage system [1, 3]. Ultimately, this modification provides the niosomes with an added time in vivo to search for its target sites, before being removed by macrophages [3, 24].

Herein, we present our results regarding the modification of niosomes by both PEGylation and magnetization. To the best of our knowledge, although PEGylation of niosomes have been well studied [12, 23, 24], and also recently, their magnetization had been tested [14], this is the first report about preparation and functional characterization of PEGylated magnetic niosomes. Carboplatin, a currently most used antitumor [25], was used to assess this system. First, PEGylated-niosomes were synthesised based on Span-60/Tween-60. Magnetic NPs were also synthesized and were then integrated into the niosomes as a mean for magnetizied drug delivery. Afterwards, these niosomes were examined on the basis of morphology, zeta potential, and magnetic particle contents. The entrapment efficiency for both NPs and Carboplatin as well as the in vitro drug release rate of these niosomes were studied. At the end, the inhibitory effect of these modified niosomes, which were loaded with Carboplatin, on MCF-7 breast cancer cell line was investigated in the presence or absence of an external magnetic field.

Materials and methods

Materials and reagents

Polyethylene glycol (PEG), ferrous chloride tetra hydrate ($FeCl_2.4H_2O$), ferric chloride hexa hydrate ($FeCl_3.6H_2O$), and NaOH were obtained from Sigma Chemical Co. (St. Louis, USA). Tween-60, Span-60, Cholesterol, 3-(4, 5-dimethylthiazol-2 yl)-2, 5-diphenyltetrazolium bromide (i.e. MTT reagent), and Tetraethyl Orthosilicate (TEOS) were obtained from Sigma-Aldrich (Madrid, Spain). Phosphate buffered saline (PBS) along with distilled water were acquired from Gibco (San Diego, US). For the in vitro experiments, neodymium magnets (0.4 Tesla) were used. All the other reagents were of analytical grade.

Synthesis of the silica-coated magnetic NPs

Magnetic Fe_3O_4 NPs were synthesised by co-precipitation method from iron (II) chloride and iron (III) chloride solutions using aqueous ammonia solution. The NPs were then washed with alcohol and rinsed with distilled water until pH 7.0 was reached. Next, the $Fe_3O_4@SiO_2$ NPs were prepared by coating of Fe_3O_4 particles with silica. Briefly, Fe_3O_4 magnetic NPs suspension (50 mL; containing 0.5 g particles) was transferred to a flask, and then, 10% aqueous Tetraethyl Orthosilicate (25 mL) was added to the flask together with alcohol (40 mL). After thouroughly mixing these reagents, the pH of the resulted suspension was set to 9.0 by adding solid NaOH. It was subsequently heated to 90 °C, and was kept at the same temperature for another 8 h stirring. After cooling the prepared suspension down to the room temperature, it was rinsed twice with alcohol and then seven times with water. The final volume was set to 70 mL with distilled water.

Characterization of the magnetic NPs

After preparation of magnetic NPs, their crystal structures were analyzed by X-ray diffraction (XRD) (Panalytical, Netherlands). Then, Fourier transform infrared spectroscopy (FTIR) was used to further investigated the molecular structure of NPs. This was accomplished by using a Fourier transform spectrometer (Bruker, Germany) at 25 °C. The magnetic properties of samples were also measured using a vibrating sample magnetometer (VSM) (Danesh Pajohan Kavir, Iran). Additionally, Scanning Electron Microscopy (SEM; SBC-12, China) was used to study the morphology of these iron oxide NPs.

Preparation of magnetized niosomes and their coating with PEG

Niosomes were synthesised based on the thin film hydration procedure [26, 27]. A flask with round bottom was used for their preparation. Briefly, cholesterol as well as Tween-60 and Span-60 surfactants were dissolved in chloroform, with a final surfactant concentration of 200 μM. Chloroform was then compeletly evaporated under the reduced pressure by a rotary evaporator (Laboroa 4003, Germany) at 60 °C for 2 h. Thin films were then hydrated by adding 5 mL of Carboplatin (1 mg/mL) along with the same volume of ferrofluid solution (5.38×10^{-7} M) at 60 °C with constant stirring for 30 min. Afterwards, the dispersions were left overnight at 25 °C to equilibrate, and then for the PEGylation of niosomes, PEG 6000 **(**5% *w*/w**)** was added. Next, small uni-lamellar niosomes were accrued from the multi-lamellar vesicles in an ultrasonic water bath at 50 °C for 30 min. Unencapsulated drug and magnetic NPs were separated from encapsulated ones by centrifugation at 7000 g for 15 min. A final purification step was performed by three times passing the niosomal suspensions across filter membranes with 400 and 200 nm pore sizes (Sartorius AG, Germany).

Physical characterization of the PEGylated magnetic niosomes

The size, zeta potential, and the polydispersity index (PDI) of niosomes were assessed by Dynamic Light Scattering (DLS) (Malvern, UK) at 25 °C through measuring the auto-correlation function. Each experiment was performed in triplicate. In addition, the morphology of the niosomal preparations was investigated by SEM (SBC-12, China) using standard procedures.

Analysis of the entrapment efficiency of niosomes

Measurement of the entrapment efficiency for magnetic NPs

For calculating the entrapment efficiency (EE%) of niosomes for magnetic NPs, concentration of ferric ions in solution were measured by *o*-phenanthroline reagent as described before [28]. Briefly, purified niosomes (100 μL) were mixed with equal volume of methanol solution (7%, *v*/v). Then, by adding 1.5 mL of 2 M HCl, magnetic materials were ionized. Next, ferric ions were reduced by adding 1 mL of 1.5 M hydroxylamine hydrochloride. Half an hour later, this mixture was supplemented with 2 mL of 11 mM *o*-phenanthroline. The resulted suspension was then mixed with 1.25 mL of 14 M NaOH, and its pH-value was set to 4.5 by citrate buffer (45 mM). Eventually, the entrapment efficiency was calculated by measuring the 510 nm absorbance values.

Measurement of the entrapment efficiency for carboplatin

The Carboplatin entrapment efficiency is expressed here as the fraction of Carboplatin traped in the niosome vesicles compared to the total amount of Carboplatin that was existed in the non-purified niosome samples [27]. First, 1 mL of each niosome formulations was diluted into 25 mL of methanol. Afterwards, the absorbance of this test solution was recorded at 260 nm, where Carboplatin displays a maximum absorption peak [29]. The methanol's role here was to break the niosomal membranes and to allow the encapsulated drug be released. Experiments were carried out in triplicate.

Investigation of the in vitro drug release from modified niosomes

A dialysis tube (Spectra/Por, 12–14 kDa cut off) was used to filled with the Carboplatin-loaded niosomes, and before use, these niosomes were treated essentially as described before [30]. After that, niosome samples were placed inside a container containing 50 mL of PBS buffer (pH 7.4). The resulting solutions were incubated at 37 °C while being stirred gently. At defined time intervals, samples were taken and characterized by examining the 260 nm absorbance. The obtained results were reported as the mean values of three measurements.

Assessing the effectiveness of the drug loaded modified niosomes towards MCF-7 cell line

The lethal effects of niosomal preparations on a breast cancer cell line, MCF-7, were investigated using MTT assay, as described before [31]. Briefly, free medium (100 μL) or equal volume of the medium contained niosomal formulations (at 2.5 μM concentration) were added to the wells of a 96-well cell culture plate at a confluency of 80% for MCF7 cells. The plate was then incubated in an incubator with humidified atmosphere of 5% CO_2 at 37 °C for 24 h. Afterwards, 15 μL of MTT reagent (Sigma; 4 mg/mL) was added to each well. The plate was then incubated in the same condition for another 4 h. Next, DMSO (100 μL) was added to each well. After another 2 h of incubation, the 490 nm absorbance of the niosome-treated as well as control wells were recorded using an ELISA Reader (FACSCalibur, US). Finally, the toxicity (T%) of the prepared formulations towards the MCF-7 cell line was then calculated based on this formulation:

$$T\% = [1 - Abs(n)/Abs(c)\,] \times 100$$

Where Abs(c) and Abs(n) are the absorbance of the control and the niosome-treated wells, respectively. Values are reported as the mean for three experiments ± standard deviation. For these tests, 0.4 Tesla neodymium magnets were used.

Statistical analysis

One-way ANOVA [32] was used for statistical analysis of different experiments. To examine the ANOVA test, a posterior Bonferroni t-test was performed. A p value <.05 was considered significant. All values are reported as the mean ± standard deviation.

Results and discussion

Niosomes are gaining attention as a replacement of liposomes in various biochemical and pharmaceutical applications. [1, 2]. In terms of drug delivery, performance of niosomes in vivo is mainly similar to that of liposomes. They both increase the circulation time of the encapsulated drugs and deliver them to their sites of action [1, 33, 34]. Although the niosomes offer a better stability [11], but their efficiencies are limited by their lower bioavailability and also fast removal from body. This lower efficiency is due to the fact that niosomes would have less time available to find and reach the tumor site before being removed. Therefore, a combined

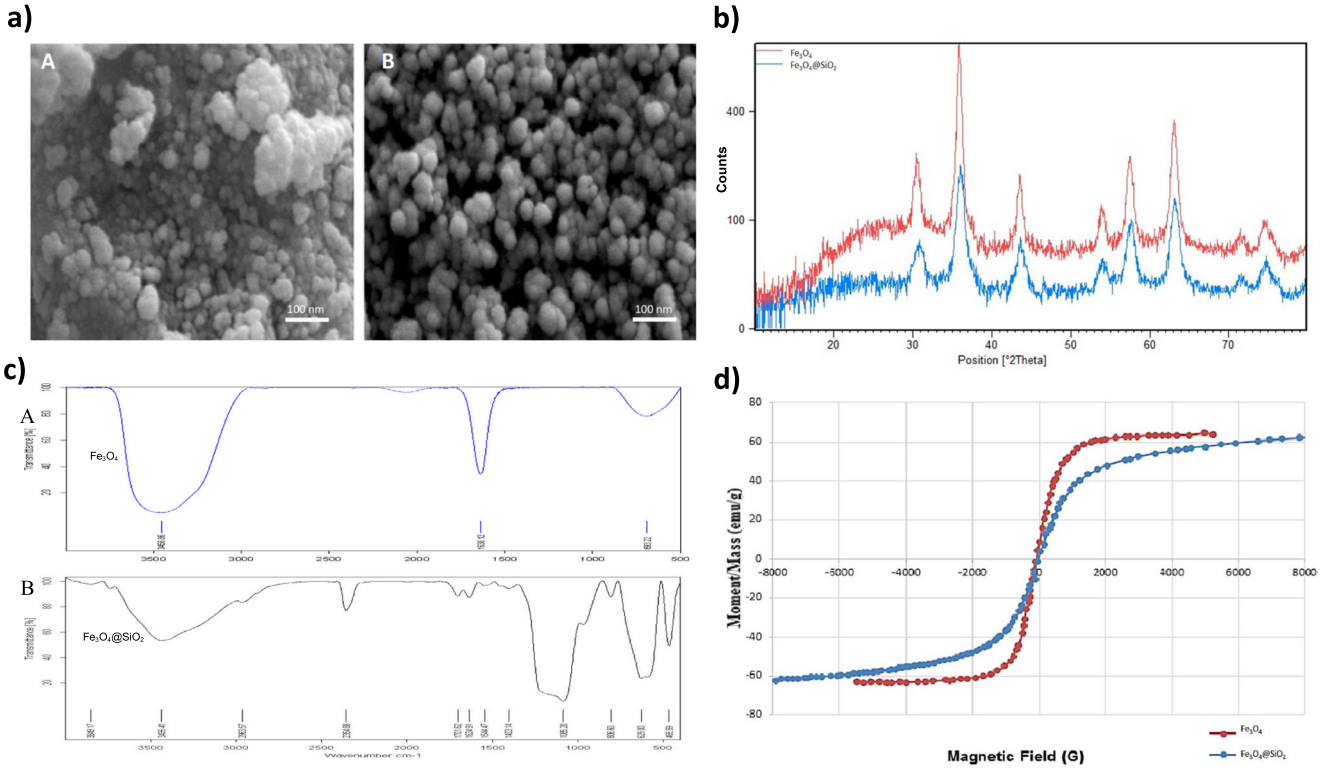

Fig. 1 Characterization of the magnetic NPs. Analysis and comparison of the synthesized NPs (Fe_3O_4 and Fe_3O_4@SiO_2) are presented. **a** SEM analysis of the magnetic NPs; panel A is Fe_3O_4 and panel B is Fe_3O_4@SiO_2 particles. **b** XRD pattern of both Fe_3O_4 (top/red pattern) and Fe_3O_4@SiO_2 (bottom/blue pattern). **c** FTIR spectrum of Fe_3O_4 (top) and Fe_3O_4@SiO_2 (bottom). **d** VSM analysis of the iron oxide NPs

approach was proposed for addressing this problem. First, by prolonging the circulation time of niosomes inside the body by PEGylation, and second, by loading of the prepared niosomal carriers with magnetic NPs. This form of delivery is compatible with biological systems, and should further increase the efficiency of the niosome based drug delivery tactics. Thus, on the one hand, the added hydration of vesicles by PEGylation would inhibit the attachment of plasma proteins [35], and consequently, will inhibit the removal of niosomal particles by macrophages [3, 13]. On the other hand, using a magnetic targeted delivery tactic can also lead to an increased local concentration of the drug. Taken together, this would result in an improvement in the efficiency of niosomes in cancer therapy.

Preparation and characterization of the magnetic NPs

Analysis of NPs by SEM: The SEM analyses of the magnetic NPs, which are presented in Fig. 1a, revealed a homogeneous morphology in both samples. They both roughly had a spherical appearance and a porous structure. Fe_3O_4@SiO_2 particles had a larger size and a more spherical morphology than Fe_3O_4 NPs (Fig. 1a) due to the presence of the SiO_2 shell. The silica shell stabilized the iron oxide NPs and prevented their agglomeration [21]. The following XRD, FTIR, and VMS analysis of these magnetic NPs revealed that they have good properties for drug delivery applications (Figs 1b, c and d).

XRD pattern: XRD was employed to further study the NPs (Fig. 1b). The XRD patterns show a unique spinel structure

Table 1 Characterization of niosomal formulations

Name	Size (nm)	PDI *	Zeta Potential (mV)	EE% * (NPs)	EE% * (Drug)
Niosomes	118.9 ± 2.1	0.37 ± 0.02	−19.5 ± 0.6	–	–
PEGylated-Niosomes	121.5 ± 1.2	0.21 ± 0.02	−14.3 ± 1.1	–	–
Niosomes/D *	127.1 ± 2.1	0.32 ± 0.01	−18.8 ± 1.2	–	73 ± 1.1
Niosomes/D + M *	129.5 ± 3.6	0.31 ± 0.06	−19.3 ± 0.7	94 ± 2.3	84 ± 1.5
PEGylated-niosomes/D	138.2 ± 0.3	0.23 ± 0.04	−16.6 ± 0.7	–	87 ± 1.6
PEGylated-niosomes/D + M	145.2 ± 1.3	0.24 ± 0.02	−15.2 ± 0.3	90 ± 2.1	83 ± 1.2

* **PDI** = polydispersity index; **D** = drug (Carboplatin); **M** = magnetic NPs (Fe_3O_4@SiO_2); and **EE%** = entrapment efficiency

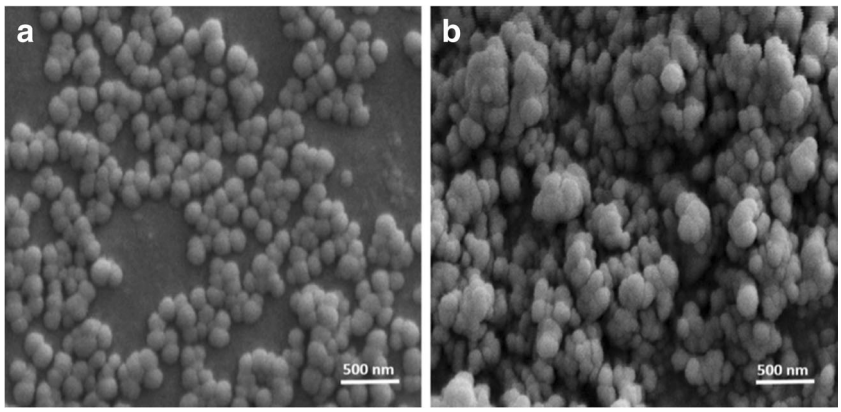

Fig. 2 Comparison of two niosomal preparations by SEM. (**Panel A**) PEGylated-niosomes containing both Carboplatin and magnetic NPs, and (**Panel B**) Naked-niosomes loaded with Carboplatin and magnetic NPs

corresponding to the magnetite Fe_3O_4 phase, where the majority of grain sizes are around 14–18 nm and 24–28 nm for Fe_3O_4 and Fe_3O_4@SiO_2 particles, respectively. As shown in Fig. 1b, it is evident that the Fe_3O_4@SiO_2 magnetic NPs have an XRD pattern very similar to that of Fe_3O_4 particles – mainly since the presence of the SiO_2 layer does not alter the crystalline structure of Fe_3O_4.

FTIR analysis of the magnetic NPs: The FTIR spectrum of Fe_3O_4 and Fe_3O_4@SiO_2 magnetic NPs are presented in Fig. 1c. Both spectra show peaks at around 600–700 cm-1, which were assigned to the Fe-O bonding vibrations. The presence of the SiO_2 layers in the spectrum of Fe_3O_4@SiO_2 NPs can be observed by the stretching vibrations of Si–O–Si and Fe–O–Si at 1097 cm^{-1} and 1085 cm^{-1}, respectively (Fig. 1c - bottom). These data strongly suggests that the Fe_3O_4@SiO_2 NPs are indeed coated with SiO_2 layers. Moreover, the peaks that are seen at 3435 cm-1 and 1634 cm-1, respectively, correspond to the O–H bonding vibrations and H–O–H bending of the magnetic NPs.

Vibration Saturation Magnetization (VSM): The VSM responses of magnetic NPs after application of external magnetic fluxes were measured (Fig. 1d). Both VSM curves (for Fe_3O_4 and Fe_3O_4@SiO_2 NPs) revealed the ferromagnetism characteristic. Coating with silica slightly decreased the saturation magnetization of Fe_3O_4@SiO_2 (57 emu/g) compared to that of Fe_3O_4 (63 emu/g). Nevertheless, these results show that silica coating of these NPs did not significantly affect their magnetic properties.

Physicochemical properties of the PEGylated magnetic niosomes

After synthesis of niosomal preparations, their sizes, zeta potential, and polydispersity index (PDI), as well as their entrapment

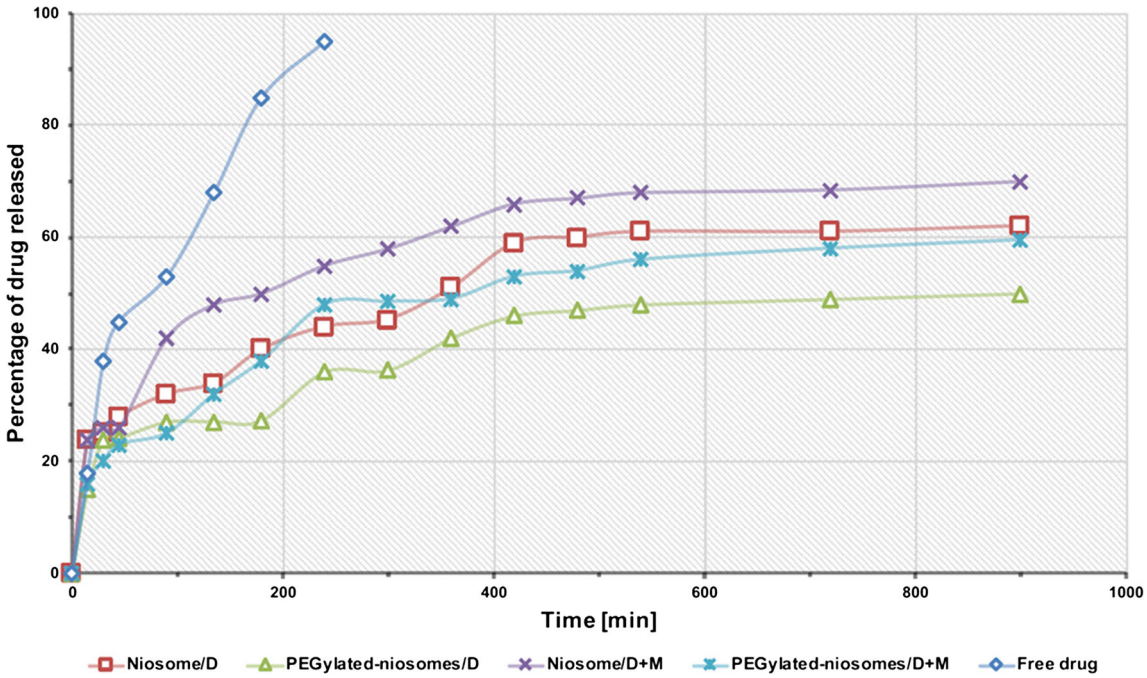

Fig. 3 The amount of drug released from different formulations over time. The cumulative release of Carboplatin from five different formulations at 37 °C over a period of 900 min is shown. **D** stands for drug (Carboplatin), and **M** is magnetic NPs (Fe_3O_4@SiO_2)

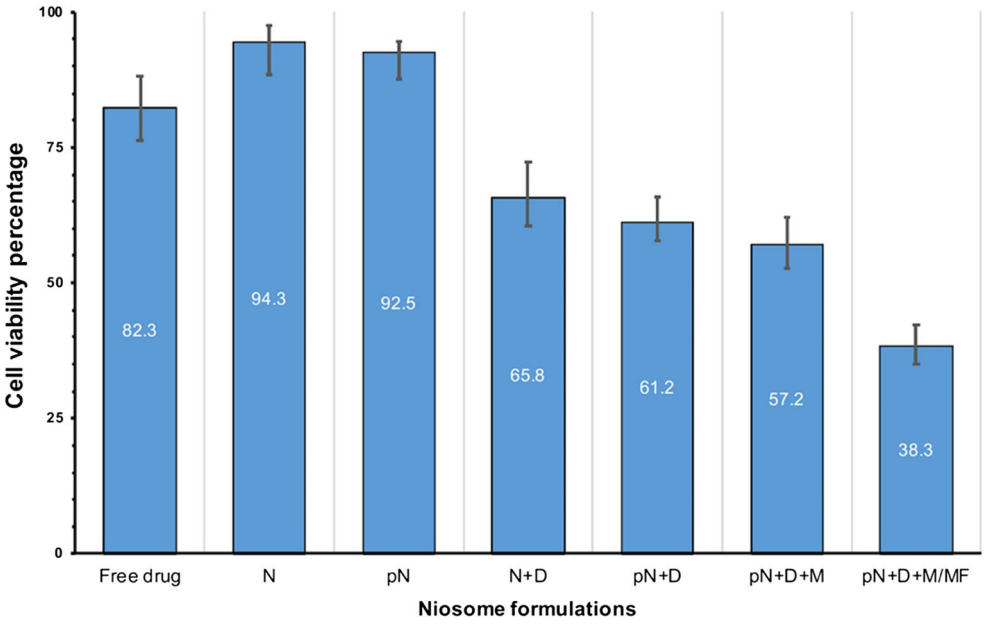

Fig. 4 Effectivness of niosomal preparations in inhibiting MCF-7 cell line. The viability of MCF-7 cancer cell line after treatment with various niosomal preparations is shown. PEGylated-niosomes loaded with drug and NPs were the most potent formulation in the presence of a magnetic field. Abbreviations: **N** represents niosomes; **pN** is the PEGylated-niosomes; **D** means drug; **M** represents the magnetic NPs, and **MF** stands for the magnetic field. Each column represents the average of three different experiments

efficiencies (EE%; for both NPs and drug) were measured (Table 1). In both naked and PEGylated-niosomes, addition of NPs and drug resulted in a slight increase in the size, however, it did not notably affect their zeta potential. Overall, the PEGylated-niosomes were larger, had a smaller negative zeta potential, and had a better PDI than the naked-niosomes. Lower negative zeta potential in PEGylated-niosomes could be due to the effects of PEG coating on the surface of niosomes. The observation of a decrease in zeta potential and an increase in size of PEGylated-niosomes, is another evidence for the immobilization of PEG molecules on the surface of niosomes.

A clear decrease in PDI from about 0.37 to 0.21 was observed when PEG was used for the coating of niosomes (Table 1). The PDI values below 0.35 show more stable and homogenous emulsions, and smaller numbers represent more uniform samples [36]. The presence of the long arm chains of PEG molecules would possibly result in further repulsion between niosomes, which prevents their agglomeration, and should therefore lead to more stability. A stability test of niosomes after 6 months confirmed this hypothesis (data not shown). This test showed that PEGylated-niosomes are more stable - their sizes changed only from 121 nm to 129 nm whereas the size of naked-niosomes changed from 118 nm to 157 nm during this longer period of time.

Afterwards, both PEGylated and naked-niosomes that have been loaded with both drug and magnetic NPs were examined with SEM (Fig. 2). They both have a spherical morphology with a good size distribution. However, as shown here, PEGylated-niosomes are larger in size, have a more spherical shape with a better dispersity than the naked-niosomes. These results are in a good agreement with the DLS analysis presented in Table 1.

Subsequently, the entrapment efficiency (EE%) of niosomes for both magnetic NPs and drug was measured. Entrapment efficiency of the naked and PEGylated-niosomes for NPs is almost similar, however, the entrapment efficiency for drug only was higher in PEGylated-niosomes ($73 \pm 1.1\%$ for naked and $87 \pm 1.6\%$ for PEGylated-niosomes) (Table 1). This better efficiency of PEGylated-niosomes could be due to the larger size of these niosomes. The presence of long chain arms of PEG may also be involved in the interaction and efficient immobilization of the drug on the surface or at the center of these surface modified niosomes.

Investigation of the in vitro drug release

Next, we sought to investigate the rates of drug release from various niosome preparations. As shown in Fig. 3, the profiles of drug released from all niosomal formulations show a biphasic pattern. This pattern consist of a first rapid release period, where around 50% of the drug are released within the first 150 min, followed by a subsequent slower and sustained release in the next 750 min. Additionaly, although, the presence of magnetic NPs lead to a facilitated release of drug from formulations, PEGylation of these niosomes (that contained both drug and magnetic particles) lead to a slower release than that of naked-niosomes containing both drug and magnetic particles ($p < .018$). The effect of PEGylation on improving the kinetics of drug release from niosomes is in agreement with the previous studies [12, 23, 24]. Furthermore, the pattern of drug release form PEGylated-niosomes containing both drug and magnetic particles was somehow equivalent to that of naked-niosomes loaded with the drug only.

In vitro effectiveness of the niosomal formulations towards MCF-7 cancer cell line

The effectiveness of the prepared niosome formulations that were loaded with Carboplatin were examined in vitro toward MCF-7, which is a well-studied breast cancer cell line, by using MTT assay. Carboplatin is a broad spectrum anticancer currently being used in chemotherapy, against ovarian carcinoma, lung, and neck cancers as well as other cancers including osteogenic sarcoma, endometrial, and breast cancers [25, 37, 38]. However, this drug has serious side-effects, including bone marrow depression and hemolytic anemia [39]. As a result, the successful implementation of niosomal magnetic delivery method is a desired approach to lessen the side effects of Carboplatin. Fig 4 shows the results obtained after treatment of MCF-7 cell line with different niosomal formulations at concentrations of 2.5 μM for 24 h. As it can be seen, none of the formulations without drug had any significant effects, however, when the drug was loaded in these formulations, the effectiveness of drug increased notably. Moreover, the effect of an external magnetic field on the viability of MCF-7 cell line was investigated. After applying the external magnetic field on niosomes containing magnetic NPs (i.e. pN + D + M/MF formulation in Fig. 4), the viability decreased to 38% compared to a 57% decrease in formulations that did not receive the external magnetic field treatment (i.e. pN + D + M formulation in Fig. 4) ($p < .001$). Taken together, these results indicate that PEGylated magnetic niosomes in the presence of an external magnetic field have a satisfactory toxicity towards the target cancer cell line.

Conclusion

In this study, we used magnetic nanoparticle for the targeted drug delivery and PEG coating for better blood distribution and stability of niosomes. An increase in size and decrease in zeta potential was seen by a coating of PEG on the surface of niosomes. PEGylation improved drug entrapment and resulted in a sustained release of Carboplatin. Moreover, using an external magnetic field greatly increased the toxicity of formulations towards cancerous cells. This promising novel drug targeting system can be used for delivery of other anticancer drugs and active agents, and could potentialy promote them as effective functional materials for magnetically controlled cancer therapy.

Compliance with ethical standards

Conflict of interest We confirm that there are no known conflicts of interest associated with this manuscript.

References

1. Moghassemi S, Hadjizadeh A. Nano-niosomes as nanoscale drug delivery systems: an illustrated review. J Control Release. 2014;185:22–36. https://doi.org/10.1016/j.jconrel.2014.04.015.
2. Nematollahi MH, Pardakhty A, Torkzadeh-Mahani M, Mehrabani M, Asadikaram G. Changes in physical and chemical properties of niosome membrane induced by cholesterol: a promising approach for niosome bilayer intervention. RSC Adv. 2017;7:49463–72. https://doi.org/10.1039/c7ra07834j.
3. Liu T, Guo R, Hua W, Qiu J. Structure behaviors of hemoglobin in PEG 6000/tween 80/span 80/H2O niosome system. Colloids Surfaces A Physicochem Eng Asp. 2007;293:255–61. https://doi.org/10.1016/j.colsurfa.2006.07.053.
4. Coviello T, Trotta AM, Marianecci C, Carafa M, Di Marzio L, Rinaldi F, et al. Gel-embedded niosomes: preparation, characterization and release studies of a new system for topical drug delivery. Colloids Surf B: Biointerfaces. 2015;125:291–9. https://doi.org/10.1016/j.colsurfb.2014.10.060.
5. Schreier H, Bouwstra J. Liposomes and niosomes as topical drug carriers: dermal and transdermal drug delivery. J Control Release. 1994;30:1–15. https://doi.org/10.1016/0168-3659(94)90039-6.
6. Bayindir ZS, Yuksel N. Characterization of niosomes prepared with various nonionic surfactants for paclitaxel oral delivery. J Pharm Sci. 2010;99:2049–60. https://doi.org/10.1002/jps.21944.
7. Priprem A, Damrongrungruang T, Limsitthichaikoon S, Khampaenjiraroch B, Nukulkit C, Thapphasaraphong S, et al. Topical Niosome gel containing an anthocyanin complex: a potential Oral wound healing in rats. AAPS PharmSciTech. 2018;19:1681–92. https://doi.org/10.1208/s12249-018-0966-7.
8. Attia N, Mashal M, Grijalvo S, Eritja R, Zárate J, Puras G, et al. Stem cell-based gene delivery mediated by cationic niosomes for bone regeneration. Nanomedicine. 2018;14:521–31. https://doi.org/10.1016/j.nano.2017.11.005.
9. Puras G, Mashal M, Zárate J, Agirre M, Ojeda E, Grijalvo S, et al. A novel cationic niosome formulation for gene delivery to the retina. J Control Release. 2014;174:27–36. https://doi.org/10.1016/j.jconrel.2013.11.004.
10. Rajera R, Nagpal K, Singh SK, Mishra DN. Niosomes: a controlled and novel drug delivery system. Biol Pharm Bull. 2011;34:945–53. https://doi.org/10.1248/bpb.34.945.
11. Kazi KM, Mandal AS, Biswas N, Guha A, Chatterjee S, Behera M, et al. Niosome: a future of targeted drug delivery systems. J Adv Pharm Technol Res. 2010;1:374–80. https://doi.org/10.4103/0110-5558.76435.
12. He RX, Ye X, Li R, Chen W, Ge T, Huang TQ, et al. PEGylated niosomes-mediated drug delivery systems for Paeonol: preparation, pharmacokinetics studies and synergistic anti-tumor effects with 5-FU. J Liposome Res. 2017;27:161–70. https://doi.org/10.1080/08982104.2016.1191021.
13. Suzuki R, Takizawa T, Kuwata Y, Mutoh M, Ishiguro N, Utoguchi N, et al. Effective anti-tumor activity of oxaliplatin encapsulated in transferrin-PEG-liposome. Int J Pharm. 2008;346:143–50. https://doi.org/10.1016/j.ijpharm.2007.06.010.
14. Tavano L, Vivacqua M, Carito V, Muzzalupo R, Caroleo MC, Nicoletta F. Doxorubicin loaded magneto-niosomes for targeted drug delivery. Colloids Surf B: Biointerfaces. 2013;102:803–7. https://doi.org/10.1016/j.colsurfb.2012.09.019.
15. Liu FR, Jin H, Wang Y, Chen C, Li M, Mao SJ, et al. Anti-CD123 antibody-modified niosomes for targeted delivery of daunorubicin against acute myeloid leukemia. Drug Deliv. 2017;24:882–90. https://doi.org/10.1080/10717544.2017.1333170.
16. Fenton O, Olafson K, Pillai P, Mitchell M, Langer R. Advances in biomaterials for drug delivery. Adv Mater. 2018;0:1705328. https://doi.org/10.1002/adma.201705328.

17. Cho K, Wang X, Nie S, Chen ZG, Shin DM. Therapeutic nanoparticles for drug delivery in cancer. Clin Cancer Res. 2008;14:1310–6. https://doi.org/10.1158/1078-0432.CCR-07-1441.
18. Liu Y, Yang F, Yuan C, Li M, Wang T, Chen B, et al. Magnetic Nanoliposomes as in situ microbubble bombers for multimodality image-guided Cancer Theranostics. ACS Nano. 2017;11:1509–19. https://doi.org/10.1021/acsnano.6b06815.
19. Chomoucka J, Drbohlavova J, Huska D, Adam V, Kizek R, Hubalek J. Magnetic nanoparticles and targeted drug delivering. Pharmacol Res. 2010;62:144–9. https://doi.org/10.1016/j.phrs.2010.01.014.
20. Park JH, Cho HJ, Yoon HY, Yoon IS, Ko SH, Shim JS, et al. Hyaluronic acid derivative-coated nanohybrid liposomes for cancer imaging and drug delivery. J Control Release. 2014;174:98–108. https://doi.org/10.1016/j.jconrel.2013.11.016.
21. Ling D, Lee N, Hyeon T. Chemical synthesis and assembly of uniformly sized iron oxide nanoparticles for medical applications. Acc Chem Res. 2015;48:1276–85. https://doi.org/10.1021/acs.accounts.5b00038.
22. Shah SA, Aslam Khan MU, Arshad M, Awan SU, Hashmi MU, Ahmad N. Doxorubicin-loaded photosensitive magnetic liposomes for multi-modal cancer therapy. Colloids Surf B: Biointerfaces. 2016;148:157–64. https://doi.org/10.1016/j.colsurfb.2016.08.055.
23. Shi B, Fang C, Pei Y. Stealth PEG-PHDCA niosomes: effects of chain length of PEG and particle size on niosomes surface properties, in vitro drug release, phagocytic uptake, in vivo pharmacokinetics and antitumor activity. J Pharm Sci. 2006;95:1873–87. https://doi.org/10.1002/jps.20491.
24. Huang Y, Chen J, Chen X, Gao J, Liang W. PEGylated synthetic surfactant vesicles (Niosomes): novel carriers for oligonucleotides. J Mater Sci Mater Med. 2008;19:607–14. https://doi.org/10.1007/s10856-007-3193-4.
25. Dasari S, Bernard Tchounwou P. Cisplatin in cancer therapy: molecular mechanisms of action. Eur J Pharmacol. 2014;740:364–78. https://doi.org/10.1016/j.ejphar.2014.07.025.
26. Bangham AD, Standish MM, Watkins JC. Diffusion of univalent ions across the lamellae of swollen phospholipids. J Mol Biol. 1965;13:IN26–7. https://doi.org/10.1016/S0022-2836(65)80093-6.
27. Tavano L, Muzzalupo R, Cassano R, Trombino S, Ferrarelli T, Picci N. New sucrose cocoate based vesicles: preparation characterization and skin permeation studies. Colloids Surf B: Biointerfaces. 2010;75:319–22. https://doi.org/10.1016/j.colsurfb.2009.09.003.
28. Kiwada H, Sato J, Yamada S, Kato Y. Feasibility of magnetic liposomes as a targeting device for drugs. Chem Pharm Bull (Tokyo). 1986;34:4253–8. https://doi.org/10.1248/cpb.34.4253.
29. Li S, Rizzo MA, Bhattacharya S, Huang L. Characterization of cationic lipid-protamine–DNA (LPD) complexes for intravenous gene delivery. Gene Ther. 1998;5:930–7. https://doi.org/10.1038/sj.gt.3300683.
30. Fenton RR, Easdale WJ, Er HM, O'Mara SM, McKeage MJ, Russell PJ, et al. Preparation, DNA binding, and in vitro cytotoxicity of a pair of Enantiomeric platinum(II) complexes, [(R)- and (S)-3-Aminohexahydroazepine]dichloro- platinum(II). Crystal structure of the S enantiomer. J Med Chem. 1997;40:1090–8. https://doi.org/10.1021/jm9607966.
31. Mosmann T. Rapid colorimetric assay for cellular growth and survival: application to proliferation and cytotoxicity assays. J Immunol Methods. 1983;65:55–63. https://doi.org/10.1016/0022-1759(83)90303-4.
32. Stoline MR. The status of multiple comparisons: simultaneous estimation of all pairwise comparisons in one-way ANOVA designs. Am Stat. 1981;35:134–41. https://doi.org/10.1080/00031305.1981.10479331.
33. Yingchoncharoen P, Kalinowski DS, Richardson DR. Lipid-based drug delivery Systems in Cancer Therapy: what is available and what is yet to come. Pharmacol Rev. 2016;68:701–87. https://doi.org/10.1124/pr.115.012070.
34. Deshpande PP, Biswas S, Torchilin VP. Current trends in the use of liposomes for tumor targeting. Nanomedicine (London). 2013;8:1509–28. https://doi.org/10.2217/nnm.13.118.
35. Shehata T, Kimura T, Higaki K, ichi Ogawara K. In-vivo disposition characteristics of PEG niosome and its interaction with serum proteins. Int J Pharm. 2016;512:322–8. https://doi.org/10.1016/j.ijpharm.2016.08.058.
36. Cheng Y, Lei J, Chen Y, Ju H. Highly selective detection of microRNA based on distance-dependent electrochemiluminescence resonance energy transfer between CdTe nanocrystals and au nanoclusters. Biosens Bioelectron. 2014;51:431–6. https://doi.org/10.1016/j.bios.2013.08.014.
37. Sheth S, Mukherjea D, Rybak LP, Ramkumar V. Mechanisms of Cisplatin-induced ototoxicity and Otoprotection. Front Cell Neurosci. 2017;11:338. https://doi.org/10.3389/fncel.2017.00338.
38. Apps MG, Choi EHY, Wheate NJ. The state-of-play and future of platinum drugs. Endocr Relat Cancer. 2015;22:R219–33. https://doi.org/10.1530/ERC-15-0237.
39. Chen X, Wang J, Fu Z, Zhu B, Wang J, Guan S, et al. Curcumin activates DNA repair pathway in bone marrow to improve carboplatin-induced myelosuppression. Sci Rep. 2017;7:17724. https://doi.org/10.1038/s41598-017-16436-9.